

TABLE III  
COMPARISON WITH NBS AND CSIRO RELATIVE TO THE CAPACITOR BF350-50T

Parameters	BF350-50T	SC-300 (NBS)	SC-330 (CSIRO)
Rating Voltage (kV)	350	300	330
Rating Capacitance (pF)	50	100	100
Eccentricity ( $10^{-6}$ m)	$140 \pm 15$		650
Rigidity Coefficient ( $10^{-6}$ m/N)	4.67 $\pm$ 0.11		12.5
Low-Voltage Electrode			
High-Voltage Electrode	$0.00 \pm 0.05$	1.02	
Insulating Bushing	$0.00 \pm 0.22$		1.25
$\frac{\partial f(a)}{\partial a} \Big _{a=a_0}$ ( $10^{-12}$ F/m)	2.79	52.9	27
$\frac{\partial f_2(a)}{\partial a} \Big _{a=a_2}$ ( $10^{-12}$ F/m)	2.13	52.9	27
$\Delta C_a/C$ ( $10^{-6}$ )	$0.04 \pm 0.02$	1.1	1.8

## REFERENCES

- [1] D. L. Hillhouse and A. E. Peterson, "A 300-kV compressed gas standard capacitor with negligible voltage dependence," *IEEE Trans. Instrum. Meas.*, vol. IM-22, no. 4, 1973.
- [2] J. Rungis and D. E. Brown, "Experimental study of factors affecting capacitance of high-voltage compressed-gas capacitors," *Proc. Inst. Elect. Eng.*, vol. 128, part A, no. 4, May 1981.
- [3] N. L. Kusters and O. Petersons, "The voltage coefficients of precision capacitors," *IEEE Trans. Consumer Electron.*, vol. CE-60, Nov. 1963.
- [4] W. E. Anderson, R. S. Davis, O. Petersons, and W. J. M. Moore, "An international comparison of high voltage capacitor calibrations," *IEEE Trans. Power App. Syst.*, vol. PAS-97, no. 4, pp. 1217-1223, 1978.

### Leak Detection for Transport Pipelines Based on Autoregressive Modeling

Guizeng Wang, Dong Dong, and Chongzhi Fang

**Abstract**—The detection and location of leaks in fluid transport pipelines often require flow measurements, which may be unavailable in practice. In this paper, a new leak detection method based on autoregressive modeling is proposed. It requires only four pressure measurements, two at each end of the pipeline. A leak above 0.5% can be reliably and quickly detected by analyzing the time sequences of the pressure gradient at the inlet and outlet of the pipeline. Furthermore, it can be easily implemented because the computational expenditure is small. Its effectiveness has been verified by tests on a 10 mm diameter, 120 m long experimental water pipeline.

## I. INTRODUCTION

With the development of the transport pipeline industry, more and more attention is paid to leak detection and location in operating transport pipelines. In the early stages, only some simple and

Manuscript received April 16, 1990; revised June 23, 1992. This work was supported by the National Science Fund of China.

G. Wang and C. Fang are with the Department of Automation, Tsinghua University, Beijing 100084, People's Republic of China.

D. Dong is with the Shandong Electric Testing and Research Institute, Jinan, People's Republic of China.

IEEE Log Number 9204221.

direct methods were used, such as flow balance methods [1] and acoustic methods [2]. In the early 1980's, Siebert [3] and Billman *et al.* [4] proposed methods based, respectively, on parameter identification and state observation, which can give more accurate results. However, these methods require flow rate measurements which sometimes are not available in practice. In this paper, a new method of leak detection based on autoregressive modeling is proposed. It only requires pressure measurements, and is thus more practicable in some instances.

## II. BASIC CONCEPT

Let  $Z$  be the coordinate along the transport pipeline axis and  $p$  the pressure of fluid in the pipeline. If the flow rate is constant, the relationship between the pressure and flow rate is approximately as follows:

$$p(Z_1) - p(Z_2) = CQ^2(Z_2 - Z_1) \quad (1)$$

where  $p(Z_1)$  and  $p(Z_2)$  represent pressures at positions  $Z_1$  and  $Z_2$ , respectively,  $Q$  is the flow rate, and  $C$  is a parameter. Assume that the medium in the pipeline is homogeneous; the temperature and friction coefficient do not change with coordinate  $Z$  and time  $t$ ; then  $C$  is a constant. The pressure distribution along the pipeline is shown as a solid line in Fig. 1.

Let  $p(O)$  and  $p(L)$  be, respectively, the inlet and outlet pressure measurements of a pipeline; from (1), we can get

$$\frac{p(O) - p(Z)}{p(Z) - p(L)} = \frac{Z}{L - Z} \quad (2)$$

where  $L$  is the length of the pipeline. The left side of (2) is not dependent on  $Q$ .

When a leak occurs at position  $Z^*$  in the pipeline, then the pressure profile changes to the dashed line shown in Fig. 1. In this case,  $[p(O) - p(Z^*)]/[p(Z^*) - p(L)]$  is not only related to  $Z^*$  and  $L$ , but is also dependent on the leak size as well.

In this proposed scheme, four pressure signals  $p(O)$ ,  $p(\Delta Z)$ ,  $p(L - \Delta Z)$ , and  $p(L)$  are measured at positions  $O$ ,  $\Delta Z$ ,  $(L - \Delta Z)$ , and  $L$ , respectively. A time sequence  $x_k$  can be devised as

$$x_k = \frac{p_k(O) - p_k(\Delta Z)}{p_k(\Delta Z) - p_k(L)} - \frac{p_k(L - \Delta Z) - p_k(L)}{p_k(O) - p_k(L - \Delta Z)} \quad (3)$$

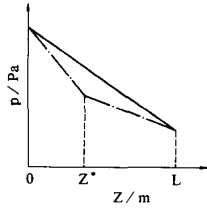


Fig. 1. Pressure distribution along pipeline.

where the subscript  $k$  implies the  $k$ th time instant. The  $x_k$  contains the information of the pressure gradients at both the upstream and downstream ends.

Note that the signal  $x_k$  is not dependent on  $Q$ , and will be equal to zero in the case when the flow rate is constant and no leak occurs in the pipeline. If there exists a stochastic disturbance in the flow process,  $x_k$  will be a random time sequence. Let  $x_k^0$  and  $x_k^1$ , respectively, represent the random time sequences acquired under normal and leaking conditions at instant  $k$ . These time sequences can be fitted to AR (autoregressive) models whose parameters and residual variances are dependent on the particular conditions of the pipeline. Leaks can be detected by using Kullback information to analyze the parameters and residual variances [5], [6].

### III. LEAK DETECTION BY USING KULLBACK INFORMATION

Kullback information is very useful in time sequence analysis.

The time sequences  $x_k^0$  and  $x_k^1$  are supposed to be stationary random sequences, and can be fitted to the following AR models[5]:

$$x_k^0 = \sum_{i=1}^m \varphi_i^0 x_{k-i}^0 + e_k^0, \quad k = 1, 2, \dots, n \quad (4)$$

$$x_k^1 = \sum_{i=1}^m \varphi_i^1 x_{k-i}^1 + e_k^1 \quad (5)$$

where  $m$  is the order of the AR model,  $e_k^j$  is a white Gaussian noise with zero mean and variance  $\sigma_j^2$ , and  $\varphi_i^j$  is the parameter of the AR model.  $j = 0, 1$  represent the normal state and leaking state, respectively, and  $n$  is the length of the time sequences.

Let the joint probability density function of  $n$ -dimensional random variables  $x_1^0, x_2^0, \dots, x_n^0$  be  $f_0(x_1, x_2, \dots, x_n)$ , and let the joint probability density function of  $n$ -dimensional random variables  $x_1^1, x_2^1, \dots, x_n^1$  be  $f_1(x_1, x_2, \dots, x_n)$ . Then the Kullback information is given by the following equation [6]:

$$I(f_0, f_1) = \frac{1}{n} \int_{-\infty}^{+\infty} \int_{-\infty}^{+\infty} \dots \int_{-\infty}^{+\infty} f_0(x_1, x_2, \dots, x_n) \cdot \ln \frac{f_0(x_1, x_2, \dots, x_n)}{f_1(x_1, x_2, \dots, x_n)} dx_1 dx_2 \dots dx_n. \quad (6)$$

Since

$$f_j(x_1, x_2, \dots, x_n) = f_j(e_n) f_j(e_{n-1}) \dots f_j(e_1),$$

therefore

$$I(f_0, f_1) = (1/n) E_0 \left\{ \ln \prod_{k=1}^n [(1/\sqrt{2\pi}\sigma_0) \exp[-(x_k - \varphi_1^0 x_{k-1} - \dots - \varphi_m^0 x_{k-m})^2 / 2\sigma_0^2]] / [(1/\sqrt{2\pi}\sigma_1) \exp[-(x_k - \varphi_1^1 x_{k-1} - \dots - \varphi_m^1 x_{k-m})^2 / 2\sigma_1^2]] \right\}$$

$$= \ln \frac{\sigma_1}{\sigma_0} - \frac{1}{2\sigma_0^2} \sum_{k=1}^n E_0 [(x_k - \varphi_1^0 x_{k-1} - \dots - \varphi_m^0 x_{k-m})^2] + \frac{1}{2\sigma_1^2} \sum_{k=1}^n E_0 [(x_k - \varphi_1^1 x_{k-1} - \dots - \varphi_m^1 x_{k-m})^2]. \quad (7)$$

$E_0$  denotes the expectation of the time sequence  $x_k^j$  with respect to  $f_0(x_1, x_2, \dots, x_n)$ :

$$E_0[(x_k - \varphi_1^0 x_{k-1} - \dots - \varphi_m^0 x_{k-m})^2] = E[(x_k^0 - \varphi_1^0 x_{k-1}^0 - \dots - \varphi_m^0 x_{k-m}^0)^2] = \sigma_0^2 \quad (8)$$

$$E_0[(x_k - \varphi_1^1 x_{k-1} - \dots - \varphi_m^1 x_{k-m})^2] = E[(e_k^0 + (\varphi_1^0 - \varphi_1^1) x_{k-1}^1 + \dots + (\varphi_m^0 - \varphi_m^1) x_{k-m}^0)^2] = \sigma_0^2 + [\Phi_0 - \Phi_1]^T R_0 [\Phi_0 - \Phi_1]. \quad (9)$$

$R_0$  is a correlation matrix, and  $\Phi_0$  and  $\Phi_1$  are parameter vectors of the AR models under their respective conditions:

$$R_0 = \begin{bmatrix} r_0(0) & r_0(1) & \dots & r_0(m-1) \\ r_0(1) & r_0(0) & \dots & r_0(m-2) \\ \dots & \dots & \dots & \dots \\ r_0(m-1) & r_0(m-2) & \dots & r_0(0) \end{bmatrix}$$

$$r_0(i) = E[x_k^0 x_{k-i}^0], \quad i = 0, 1, \dots, m-1$$

$$\Phi_0 = [\varphi_1^0, \varphi_2^0, \dots, \varphi_m^0]^T, \quad \Phi_1 = [\varphi_1^1, \varphi_2^1, \dots, \varphi_m^1]^T. \quad (10)$$

Substituting (8) and (9) into (7) yields

$$I(f_0, f_1) = \frac{1}{2} \left\{ \ln \frac{\sigma_1^2}{\sigma_0^2} - 1 + \frac{1}{\sigma_1^2} [\sigma_0^2 + (\Phi_0 - \Phi_1)^T R_0 (\Phi_0 - \Phi_1)] \right\}. \quad (11)$$

Similarly, we can get

$$I(f_1, f_0) = \frac{1}{2} \left\{ \ln \frac{\sigma_0^2}{\sigma_1^2} - 1 + \frac{1}{\sigma_0^2} [\sigma_1^2 + (\Phi_0 - \Phi_1)^T R_1 (\Phi_0 - \Phi_1)] \right\} \quad (12)$$

where  $R_1$  is a correlation matrix:

$$R_1 = \begin{bmatrix} r_1(0) & r_1(1) & \dots & r_1(m-1) \\ r_1(1) & r_1(0) & \dots & r_1(m-2) \\ \dots & \dots & \dots & \dots \\ r_1(m-1) & r_1(m-2) & \dots & r_1(0) \end{bmatrix}$$

$$r_1(i) = E[x_k^1 x_{k-i}^1], \quad i = 0, 1, \dots, m-1. \quad (13)$$

Because Kullback information does not have a symmetric property, a Kullback divergence function  $P_f = I(f_0, f_1) + I(f_1, f_0)$  is pro-

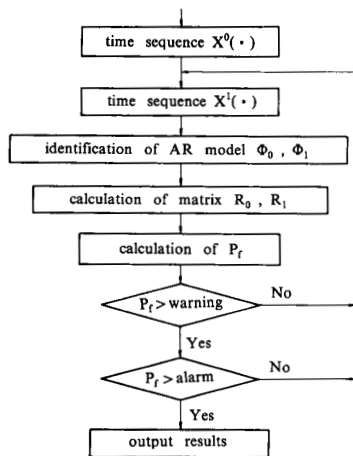


Fig. 2. Flowchart of real-time leak detection procedure.

posed as a performance index of leaking [8], [9]:

$$P_f = \frac{1}{2\sigma_1^2} \{ \sigma_0^2 + [\Phi_0 - \Phi_1]^T R_0 [\Phi_0 - \Phi_1] \} + \frac{1}{2\sigma_0^2} \{ \sigma_1^2 + [\Phi_0 - \Phi_1]^T R_1 [\Phi_0 - \Phi_1] \} - 1. \quad (14)$$

It is apparent that  $P_f \geq 0$ . When these two time sequences have the same statistical characteristics,  $P_f = 0$ . If a leak occurred,  $x_k^1$  would be different from  $x_k^0$ , and  $\Phi_1$  and  $\sigma_1^2$  different from  $\Phi_0$  and  $\sigma_0^2$ , which lead to  $P_f > 0$ .

The flowchart of a real-time leak detection procedure is shown in Fig. 2. Four steps are included.

- 1) Acquisition of time sequences  $x_k^0$  and  $x_k^1$ .
- 2) AR model identification.
- 3) Correlation function calculation. The correlation function  $r_j(i)$  is estimated by

$$\hat{r}_j(i) = \frac{1}{n} \sum_{k=0}^{n-1} x_k^i x_{k-i}^i,$$

and the recursive form of the calculation of  $r_j(i)$  is as follows [10]:

$$\hat{r}_j(i, k) = (1 - \psi)\hat{r}_j(i, k-1) + \psi(x_k^i x_{k-1}^i)$$

where  $\psi$  is a forgetting factor,  $0.9 < \psi < 1.0$ .

- 4) Calculation of  $P_f$ . It can be calculated by (14).

A leak alarm will be triggered when  $P_f$  is beyond the preset threshold.

#### IV. TEST RESULTS

The method proposed in this paper has been verified on a 10 mm diameter, 120 m long experimental water pipeline. A schematic layout of the experimental pipeline system is shown in Fig. 3. The pipeline lies horizontally. At the upstream end of the pipeline are two pumps in series. Four pressure sensors with 0.2% precision are installed at positions 0, 20, 100, and 120 m from the upstream end. Along the pipeline, there are several points which can be used to develop a leak. A microcomputer IBM-PC/XT with a 12-b A/D converter is used for data acquisition and data processing. The sampling period is set at 20 ms, the order of AR models  $m = 5$ , the length of the time sequences  $n = 2000$ , and the forgetting factor  $\psi = 0.95$ . The test results are given in Figs. 4-6. Fig. 4 shows the

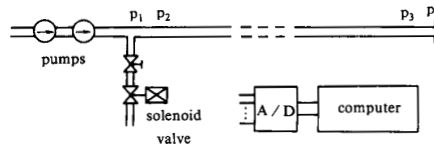


Fig. 3. Schematic layout of the experimental water pipeline system.

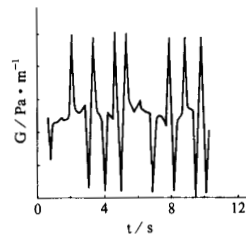
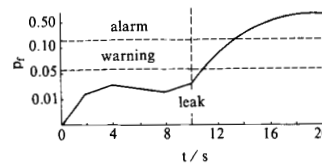
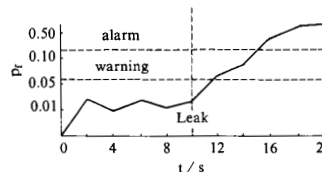


Fig. 4. Pressure gradient at upstream end.

Fig. 5. Performance index  $P_f$  versus time (1% leak).Fig. 6. Performance index  $P_f$  versus time (0.5% leak).

pressure gradient signal  $[p(0) - P(\Delta Z)]$  at the upstream end. Fig. 5 shows the performance index  $P_f$  versus time when a 1% leak occurred at  $t = 10$  s. Fig. 6 shows the performance index  $P_f$  versus time for a 0.5% leak.

#### V. CONCLUSIONS

The test results illustrate the effectiveness of the proposed leak detection method. A 0.5% leakage can be reliably and almost instantly detected by this method. Since this method does not require flow rate measurement, it is more practical in many instances. The basic idea of using autoregressive models for leak detection can be used for other fault detections as well.

#### REFERENCES

- [1] H. H. Brons and H. Schaffhausen, "European methods of leak detection and location," *Pipe Line Industry*, pp. 50-66, May 1972.
- [2] J. R. De Read, "Comparison between ultrasonic and magnetic flux pigs for pipeline inspection," *Pipes and Pipeline Int.*, pp. 7-15, Jan.-Feb. 1987.
- [3] H. Siebert, "A simple method for detection and locating leaks in gas pipeline," *Process Automation*, no. 2, pp. 90-95, 1981.
- [4] L. Billman and R. Isermann, "Leak detection methods for pipelines," in *Proc. 8th IFAC Congr.* Budapest, Hungary, 1984, pp. 381-385.

- [5] N. K. Sinha and B. Kuszta, *Modeling and Identification of Dynamic Systems*. New York: Van Nostrand Reinhold, 1983.
- [6] S. Kullback, *Information Theory and Statistics*. New York: Wiley, 1959, ch. 1, pp. 3-7.
- [7] T. Fukuda and T. Mitsuoka, "Leak detection and its localization in pipeline systems," in *Proc. IMEKO Symp. Flow Meas. Contr. Ind.* Tokyo, Japan, 1979, pp. 193-198.
- [8] O. E. Schvnichiro and T. Soeda, "A method of predicting failure or life for stochastic systems by using autoregressive models," *Int. J. Syst. Sci.*, vol. 11, pp. 1177-1188, 1980.
- [9] S. O. Y. Tomita and T. Soeda, "Failure detection and prediction system by using adaptive digital filter," in *Proc. IFAC Real Time Digital Contr. Appl. Conf.*, Guadalajara, Mexico, 1983, pp. 93-99.
- [10] R. Isermann, "Practical aspects of process identification," *Automatica*, vol. 16, pp. 575-587, 1980.

## Precision Average-Sensing AC/DC Converters

Olev Märtens and Toom Pungas

**Abstract**—Various configurations of average-sensing ac/dc converters for precision ac voltage measurements are described. Due to the unique electrical configurations in which the influence of the inaccuracy of ratio resistors is suppressed, these converters have high accuracy (better than 0.01%) and resolution (0.0001%) at medium frequencies. Their frequency range is from 10 Hz to 1 MHz, with a settling time less than 1 s.

### I. INTRODUCTION

Conventional average-sensing ac/dc converters include a half-wave or a full-wave operational rectifier and a low-pass filter. Conversion is achieved there by switching resistors in the negative feedback path of an operational rectifier (for example, by diode switches) to obtain +1 and -1 gains during positive and negative half-waves [1]. The main disadvantage of such converters is that the conversion accuracy directly depends on the accuracy of resistor ratios. These converters are also quite complex, as they include a low-pass filter and often a means to suppress the offset voltage.

ac/dc conversion may also be performed using the idea of switching a capacitor (capacitors) in the negative feedback path of an op-amp. In such converters, due to circuit asymmetry for both half-waves, direct voltage is generated on a capacitor (capacitors), proportional to the input ac signal [2], [3].

The idea of switching capacitors makes it possible to design average-sensing ac/dc converters, which perform the conversion of the input alternating voltage into alternating current, and the conversion of the rectified current into output direct voltage on the same resistors. The transfer errors of these converters depend weakly on the resistor ratio errors.

### II. PROPOSED AC/DC CONVERTERS

#### A. Half-Wave Converter

The half-wave ac/dc converter is shown in Fig. 1. The ac input voltage drops on the input resistor  $R_2$  because the other end of  $R_2$

Manuscript received February 19, 1992; revised May 19, 1992.  
O. Märtens is with Enari Electronics Ltd., Pronski str.52-11, Tallinn, EE 0010, Estonia.  
T. Pungas is with Estonian Association of Inventors, Toompuiestee str.7, Tallinn, EE 0110, Estonia.  
IEEE Log Number 9204222.

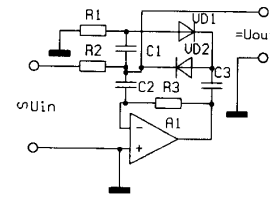


Fig. 1. A half-wave ac/dc converter.

is at the virtual ground potential, connected via the capacitor  $C_2$  to the inverting input of the op-amp  $A_1$ . The negative feedback path includes the capacitor  $C_3$ , the diode  $VD_1$ , and the capacitor of  $C_1$ , during the positive half-waves of the input signal, or the diode  $VD_2$ , during the negative half-waves. The input bias current of the op-amp may be neglected because its ratio to the nominal value of the rectified current is smaller than  $1/1\,000\,000$ ; the alternating current in  $R_2$  must flow to the output of the amplifier, and is rectified by  $VD_1$  and  $VD_2$ . The direct component of the current flowing through  $VD_2$  may flow only through  $R_2$ , as the rest of the circuit is separated by  $C_2$  and  $C_3$ . In effect, the dc voltage drop on the resistor  $R_2$  is proportional to the average value of the rectified input voltage.

The transfer coefficient of this converter is

$$K = (U_{out}/U_{in}) = 0.5 \quad (1)$$

where  $U_{out}$  is the value of the output direct voltage, and  $U_{in}$  is the average value of the rectified input ac voltage.

Resistor  $R_3$  in this configuration, as well as in the following configurations, is providing the operation of the op-amp at dc. This resistor must have a large value, as for ac it is switched in parallel to the reverse resistances of the diodes.

High accuracy and stability of the transfer coefficient of this converter are achieved by converting the input ac voltage into the ac current, and converting the rectified current into the output dc voltage on the same resistor. An advantage of this converter is also suppression of the ripple voltage by the converter itself because for the ac, the inverting input of the op-amp is connected to the output of the converter. The circuit has no offset error because the op-amp works as an ac amplifier only, and is fully separated by capacitors from the output.

#### B. Full-Wave Rectifier

The full-wave converter shown in Fig. 2 works in a similar way. However, the transfer coefficient of this converter is higher, as the rectified ac current is not determined by the conductance of one resistor, but by the conductance of two resistors  $R_1$  and  $R_2$  connected in parallel. The output direct voltage is generated on the capacitor  $C_2$ , and the transfer coefficient is determined by the ratio of the resistor  $R_2$ , on which the rectified current generates the output voltage, to the parallel resistance of  $R_1$  and  $R_2$ . The transfer coefficient of this converter is

$$K = (U_{out}/U_{in}) = 0.5 * (1 + R_2/R_1). \quad (2)$$

If the resistors  $R_1$  and  $R_2$  have the same nominal values, then the resistor ratio may be expressed using the value of the relative inaccuracy of the ratio  $R_2/R_1$ :

$$R_2/R_1 = 1 + \delta r. \quad (3)$$